CIA Open Access

Comparative Analysis of Unsupervised Learning Approaches for Anomalous Billing Pattern Detection in Healthcare Payment Integrity

Xiaotong Shi[1], *Haojun Weng*[1.2]

[1] *Business Analytics, Columbia University, NY, USA*
[1.2] *Computer Technology, Fudan University, Shanghai, China*

DOI: 10.63575/CIA.2024.20110

Abstract

Healthcare payment integrity faces substantial challenges from anomalous billing patterns that undermine financial sustainability and compromise resource allocation effectiveness. This research develops a systematic comparative framework evaluating five unsupervised learning algorithms—Isolation Forest, Local Outlier Factor, DBSCAN, One-Class SVM, and Autoencoder—for detecting aberrant billing behaviors within medical claims databases. Through empirical analysis of Medicare Part B data spanning 142,738 provider records, we quantify detection accuracy, computational efficiency, and pattern recognition capabilities across distinct algorithmic approaches. Isolation Forest demonstrates superior performance with 0.847 F1-score and 3.2-second processing time per 10,000 claims, while Autoencoders reveal 23.6% higher sensitivity to complex multivariate anomalies. The analysis identifies critical tradeoffs between precision-recall balance and scalability constraints, establishing quantitative benchmarks for algorithm selection in operational fraud detection systems. Our findings indicate that ensemble configurations combining density-based and reconstruction-error methodologies yield 15.8% improvement over single-algorithm deployments.

Keywords: *Healthcare payment integrity, Unsupervised learning, Anomaly detection, Billing pattern analysis*

1. Introduction

1.1. Background and Motivation of Healthcare Payment Integrity

Healthcare expenditure constitutes a substantial economic burden across global health systems, with fraudulent activities and billing irregularities accounting for approximately 3-10% of total healthcare spending annually. Within the United States Medicare program alone, improper payments reached $31.2 billion in fiscal year 2023, representing persistent vulnerabilities in payment integrity mechanisms. These financial losses extend beyond direct monetary impact, disrupting resource allocation for legitimate medical services and eroding public trust in healthcare financing systems. Medical billing fraud manifests through diverse patterns including upcoding procedures to higher reimbursement categories, billing for services never rendered, unbundling procedural codes to maximize payment, and phantom billing where providers submit claims for fictitious patients.

Traditional rule-based detection systems rely on predetermined thresholds and manually crafted heuristics, creating rigid frameworks incapable of adapting to evolving fraudulent tactics. Manual auditing processes consume extensive investigative resources while examining merely 1-3% of submitted claims, allowing sophisticated fraud schemes to persist undetected for prolonged periods. The exponential growth of electronic health records and claims databases generates massive data volumes exceeding human analytical capacity, necessitating automated detection methodologies capable of identifying subtle anomalies within millions of transactions. Payment integrity programs require methods that balance detection sensitivity with operational feasibility, minimizing false positive rates that burden compliant providers with unnecessary investigations while maintaining sufficient vigilance to capture genuine fraudulent activities.

Machine learning approaches offer adaptive capabilities for recognizing complex patterns within high-dimensional claims data without requiring explicit programming of fraud indicators. Unsupervised learning techniques prove particularly valuable in this domain where labeled fraud instances remain scarce, expensive to obtain, and subject to selection bias from previously detected cases. These algorithms identify statistical outliers and unusual behavioral patterns by learning normal claim distributions from unlabeled data, enabling discovery of novel fraud schemes not anticipated by rule designers. The application of multiple unsupervised methodologies allows healthcare organizations to leverage complementary detection mechanisms, capturing different anomaly types through varied mathematical frameworks.

1.2. Challenges in Anomalous Billing Pattern Detection

Healthcare claims data presents unique analytical challenges stemming from extreme dimensionality, class imbalance, and heterogeneous feature types. Medical billing records incorporate hundreds of potential features including provider specialty codes, procedure codes from Current Procedural Terminology (CPT) nomenclature, diagnosis codes from International Classification of Diseases (ICD) taxonomy, patient demographics, geographic indicators, and temporal patterns. This high-dimensional feature space creates computational complexity for distance-based algorithms while introducing curse of dimensionality effects that degrade anomaly separation in many traditional methods. Claims datasets typically contain 99.5% or more legitimate transactions, creating severe class imbalance where anomalous patterns represent rare events easily overwhelmed by normal claim distributions.

Feature engineering requires domain expertise to transform raw billing codes into meaningful representations capturing fraud indicators. The categorical nature of medical codes presents challenges for algorithms designed around continuous numerical features, necessitating encoding strategies that preserve semantic relationships between similar procedures or diagnoses. Temporal dependencies exist where fraud patterns evolve across claim submission sequences, requiring methods capable of detecting both point anomalies in individual claims and collective anomalies across provider behavior portfolios. Privacy regulations including Health Insurance Portability and Accountability Act (HIPAA) constraints limit data sharing and restrict algorithm development to proprietary datasets, hindering reproducibility and benchmarking across research studies.

Evaluation metrics face complications from the absence of comprehensive ground truth labels. Real fraud cases identified through investigations represent only detected instances, potentially excluding undetected fraudulent activities from validation sets. Performance assessment must balance multiple objectives including detection sensitivity, false positive minimization, computational efficiency, and interpretability for investigative workflows. Operational deployment requires algorithms to process claims in near-real-time within existing infrastructure constraints, demanding scalability to millions of transactions while maintaining detection accuracy. The dynamic nature of fraudulent behaviors necessitates continuous model updates as perpetrators adapt tactics to circumvent detection systems.

1.3. Research Objectives and Contributions

This research establishes a quantitative comparative framework for evaluating unsupervised learning algorithms applied to healthcare billing anomaly detection. We implement five distinct algorithmic approaches spanning density-based methods, distance-based techniques, clustering algorithms, boundary-based classifiers, and neural network architectures. Through controlled experimentation on standardized Medicare claims data, we measure performance across multiple dimensions including detection accuracy metrics, computational resource consumption, scalability characteristics, and anomaly pattern interpretability. The analysis identifies specific algorithmic strengths and weaknesses relative to different fraud manifestations, enabling evidence-based selection criteria for operational deployment scenarios.

Our experimental design addresses methodological gaps in prior comparative studies by standardizing preprocessing pipelines, feature engineering strategies, and evaluation protocols across all tested algorithms. We quantify tradeoffs between precision and recall through comprehensive receiver operating characteristic analysis, establishing optimal operating points for different organizational risk tolerances. Computational efficiency measurements provide practical guidance on infrastructure requirements and processing throughput capabilities. The research examines algorithm sensitivity to hyperparameter configurations, documenting robustness across parameter variations. We analyze detected anomaly characteristics, correlating algorithmic findings with known fraud taxonomies to assess detection mechanism effectiveness.

The contribution framework encompasses three primary dimensions. We provide empirical performance benchmarks establishing quantitative baselines for five major unsupervised learning paradigms applied to healthcare billing data under controlled experimental conditions. The analysis generates actionable insights regarding algorithm selection criteria based on organizational priorities such as investigation resource availability, acceptable false positive rates, and computational infrastructure constraints. We identify opportunities for ensemble configurations that combine complementary detection mechanisms, demonstrating synergistic performance improvements over individual algorithm deployments. These findings advance both academic understanding of unsupervised anomaly detection capabilities and practical implementation guidance for healthcare payment integrity programs.

2. Related Work and Literature Review

2.1. Evolution of Fraud Detection in Healthcare Systems

Healthcare fraud detection methodologies have undergone substantial transformation from manual auditing procedures to sophisticated computational approaches over the past three decades. Early detection mechanisms relied entirely on random sampling and tip-based investigations, examining small claim subsets selected through statistical sampling or reported suspicious activities. Bauder and Khoshgoftaar [1]

documented the transition toward data mining techniques in Medicare fraud analysis, demonstrating how machine learning algorithms could identify provider billing patterns deviating from peer cohorts. Their work established foundational approaches applying supervised classification to labeled fraud cases, achieving detection rates substantially exceeding random auditing baselines.

The emergence of big data analytics transformed fraud detection capabilities by enabling comprehensive analysis of entire claims populations rather than limited samples. Gomes et al. [2] investigated deep learning architectures for insurance fraud identification, developing autoencoder networks capable of learning compressed representations of normal claim characteristics. Their unsupervised approach detected fraudulent patterns without requiring labeled training data, addressing the fundamental challenge of obtaining verified fraud labels at scale. The research demonstrated that reconstruction error metrics from autoencoder models provided effective anomaly scores for ranking suspicious claims, achieving precision-recall curves superior to traditional statistical methods.

Graph-based analytical techniques emerged as investigators recognized the network structure inherent in healthcare fraud schemes involving collusion between providers, patients, and intermediaries. Van Capelleveen et al. [3] examined outlier detection methodologies specifically within Medicaid dental claims, implementing multiple unsupervised algorithms including Local Outlier Factor and Isolation Forest. Their comparative study revealed substantial performance variation across algorithms depending on data characteristics and anomaly types, with no single method dominating across all evaluation criteria. The research emphasized the importance of domain-specific feature engineering, showing that medically-informed features substantially improved detection accuracy compared to raw billing codes.

2.2. Unsupervised Learning Techniques in Medical Billing Analysis

Scoring models represent an established approach for quantifying billing pattern irregularity through composite metrics aggregating multiple fraud indicators. Shin et al. [4] developed a weighted scoring framework incorporating variables such as claim frequency deviations, unusual service combinations, and provider specialty mismatches. Their methodology assigned risk scores to individual claims and providers, enabling prioritization of investigative resources toward highest-risk entities. The scoring approach achieved interpretability advantages over black-box machine learning models, allowing investigators to understand specific factors contributing to elevated risk assessments.

Association rule mining techniques identify frequently co-occurring patterns within transaction databases, revealing suspicious billing combinations that violate expected medical practice standards. Chandola et al. [5] applied knowledge discovery methodologies to massive healthcare claims datasets, extracting patterns indicating potential abuse or fraud. Their work demonstrated how data mining could surface novel fraud schemes not anticipated by rule designers, discovering previously unknown billing patterns warranting investigation. The research established preprocessing pipelines for handling the scale and complexity of national claims databases, addressing computational challenges in pattern mining across billions of transactions.

Multidimensional analytical frameworks incorporate diverse data sources beyond basic billing records, integrating provider characteristics, patient histories, geographic patterns, and temporal trends. Thornton et al. [6] developed prediction models utilizing medical necessity indicators, provider enrollment data, and claims submission patterns to identify Medicaid fraud risks. Their research highlighted the value of feature diversity, showing that models incorporating multiple data dimensions outperformed analyses limited to billing codes alone. The study quantified how different feature categories contributed to detection accuracy, guiding feature selection strategies for operational systems.

Statistical outlier detection methods identify observations deviating significantly from expected distributions within defined peer groups. Kose et al. [7] implemented interactive machine learning systems combining automated anomaly detection with human expert feedback, creating iterative refinement workflows. Their approach recognized that fraud detection requires continuous adaptation as fraudulent behaviors evolve, necessitating systems capable of incorporating investigator insights to improve detection accuracy over time. The interactive methodology demonstrated superior long-term performance compared to static models, adapting to emerging fraud patterns through feedback loops.

2.3. Research Gaps and Opportunities in Current Approaches

Existing comparative studies exhibit limitations in experimental design rigor, often evaluating algorithms on different datasets, preprocessing pipelines, or evaluation metrics, preventing direct performance comparison. Liu et al. [8] conducted graph analysis for detecting fraud, waste, and abuse, emphasizing network-based pattern recognition. Their work revealed detection capabilities inherent in relationship structures between healthcare entities, complementing transaction-level analyses. The research identified gaps in standard approaches that analyze claims independently, missing patterns only visible through network perspectives examining provider-patient interaction graphs and referral networks.

Limited attention has focused on practical deployment considerations including computational scalability, inference latency, and model interpretability requirements for operational fraud detection systems. Roy and

George [9] examined insurance claim fraud using machine learning techniques across multiple insurance types, documenting algorithm performance variation across different claim categories. Their findings suggested that algorithm effectiveness depends substantially on domain-specific characteristics, with no universal best approach applicable across all healthcare contexts. This observation motivates comprehensive comparative analysis establishing performance baselines across standardized evaluation protocols.

The absence of standardized benchmark datasets hampers reproducibility and prevents meta-analysis synthesizing findings across studies. Bauder et al. [10] surveyed the state of healthcare upcoding fraud analysis, identifying fragmentation in research methodologies and evaluation approaches. Their review documented the prevalence of proprietary datasets inaccessible to the broader research community, limiting independent validation of reported results. The authors advocated for development of publicly available benchmark datasets enabling fair algorithm comparison and accelerating methodological advances through shared evaluation frameworks.

Class imbalance challenges receive inconsistent treatment across studies, with varying approaches to handling extreme rarity of fraudulent cases in operational datasets. Herland et al. [11] investigated fraud detection using multiple Medicare data sources, demonstrating how integrating diverse information streams improved detection accuracy. Their work employed big data processing frameworks to handle the scale of national healthcare databases, establishing infrastructure patterns for analyzing claims at population scale. The research quantified performance gains from data integration, motivating multi-source analytical approaches.

Neural network applications in healthcare fraud detection remain relatively unexplored compared to traditional machine learning methods, despite demonstrated success in other anomaly detection domains. Johnson and Khoshgoftaar [12] developed neural network architectures specifically for Medicare fraud identification, exploring deep learning capabilities for capturing complex non-linear relationships in billing patterns. Their research revealed that neural approaches required substantial training data volumes to achieve competitive performance, presenting challenges in fraud detection contexts where labeled examples remain scarce. The study identified opportunities for transfer learning and pre-training strategies to enhance neural network effectiveness with limited labeled fraud cases.

Blockchain and emerging technologies present new paradigms for fraud prevention through immutable audit trails and distributed verification mechanisms. Kapadiya et al. [13] analyzed blockchain and artificial intelligence architectures for healthcare insurance fraud detection, proposing frameworks integrating multiple technological approaches. Their work examined how blockchain could address data integrity concerns while AI algorithms provided analytical detection capabilities. The research established conceptual architectures for next-generation fraud detection systems, though practical implementation and performance validation remain largely unexplored.

Recent methodological advances in deep learning and ensemble techniques have not been systematically evaluated against established baseline methods in healthcare billing contexts. Aslam et al. [14] surveyed artificial intelligence and machine learning applications for insurance fraud detection across multiple insurance domains, documenting the diversity of algorithmic approaches. Their review identified healthcare insurance as presenting unique challenges including complex coding systems, medical necessity considerations, and regulatory constraints distinguishing it from other insurance fraud contexts. The survey called for healthcare-specific methodological development rather than direct application of techniques developed for other fraud types.

Contemporary research increasingly emphasizes real-time detection capabilities and adaptive systems that evolve with changing fraud patterns. Prova [15] examined machine learning approaches for healthcare fraud detection, implementing multiple algorithms on standardized datasets. The study compared traditional supervised methods against unsupervised approaches, finding that unsupervised techniques achieved competitive detection accuracy while avoiding labeled data requirements. This work reinforced the practical value of unsupervised methods for operational deployment where obtaining verified fraud labels presents persistent challenges[16].

3. Methodology and Experimental Design

3.1. Dataset Description and Preprocessing Strategies

This research employs the Medicare Part B Provider Summary dataset encompassing fiscal year 2022 claims submissions from 142,738 registered healthcare providers across all U.S. states and territories, consistent with datasets utilized in prior Medicare fraud studies. The dataset aggregates billing information at provider level, containing 89 distinct features capturing service volumes, procedure distributions, payment amounts, and beneficiary demographics [17]. Each provider record represents accumulated claims activity over the annual period, with individual providers submitting between 11 and 847,293 claims depending on practice size and specialty[18]. The dataset includes both inpatient and outpatient service categories, covering medical procedures, diagnostic services, durable medical equipment, and pharmaceutical provisions[19].

Raw data contains multiple challenges requiring systematic preprocessing before algorithm application. Missing values appear in approximately 12.7% of feature entries, primarily in optional demographic fields

and specialty subcategories[20]. We implement conditional imputation strategies based on provider type, utilizing modal values within specialty cohorts for categorical variables and median values for continuous features[21]. Extreme outliers resulting from data entry errors receive identification through statistical bounds set at 4.5 standard deviations from specialty-specific means, with outlier values replaced by cohort-appropriate substitutes[22]. The preprocessing pipeline preserves genuine anomalies representing potential fraud while eliminating artificial outliers stemming from technical issues[23].

Feature engineering transforms raw billing codes into analytically tractable representations capturing medical and financial semantics, following established preprocessing practices in healthcare fraud detection[24]. Procedure code frequencies undergo normalization relative to provider specialty baselines, generating deviation scores quantifying how substantially individual providers diverge from peer group patterns[25]. We construct composite features aggregating related procedures into clinically meaningful categories, reducing dimensionality from thousands of individual codes to 156 aggregated service groups. Geographic features incorporate regional cost adjustments and urban-rural classifications affecting expected billing patterns[26]. Temporal features capture claim submission timing patterns, identifying unusual periodicity or submission bursts potentially indicating batch fraud schemes[27].

Categorical variables including provider specialty, geographic region, and medical school training undergo encoding through multiple strategies evaluated for algorithmic compatibility[28]. One-hot encoding generates binary indicator variables for categories, creating sparse high-dimensional representations suitable for tree-based and linear models[29]. Target encoding replaces categories with statistical summaries computed over associated claims, producing continuous representations capturing category-specific behaviors[30]. Entity embedding techniques employed for neural network approaches learn dense vector representations of categorical values during model training, discovering semantic relationships between similar categories[31].

Data standardization applies feature-specific transformations addressing scale heterogeneity across variables[32]. Numerical features measuring claim volumes, payment amounts, and service frequencies undergo z-score normalization, centering distributions at zero mean with unit variance [33]. This transformation ensures equal influence across features with naturally different scales, preventing payment amounts measured in thousands of dollars from dominating distance calculations over claim counts[34]. Certain algorithms including tree-based methods remain insensitive to feature scaling, while distance-based and neural approaches require standardization for optimal performance [35]. We maintain separate preprocessing pipelines tailored to specific algorithmic requirements while preserving consistent feature sets across all methods[36].

Training and evaluation splits partition the provider population into development and test cohorts using stratified sampling based on provider specialty and claim volume categories[37]. The training set encompasses 80% of providers (114,190 records) for algorithm configuration and hyperparameter optimization, while the test set retains 20% (28,548 providers) for final performance evaluation [38]. Stratification ensures representative distributions across key provider characteristics, preventing evaluation bias from specialty imbalances. We implement 5-fold cross-validation within the training partition to assess generalization performance and tune algorithmic hyperparameters, computing performance metrics averaged across validation folds[39].

3.2. Selection and Configuration of Unsupervised Learning Algorithms

Isolation Forest Implementation

Isolation Forest operates through recursive random partitioning of feature space, isolating anomalies in fewer splits than normal observations clustered in dense regions, a mechanism particularly effective for high-dimensional healthcare data[40]. The algorithm constructs an ensemble of isolation trees, each built by randomly selecting splitting features and split values until observations separate into individual leaves. Anomalies require fewer splits to isolate due to their distance from normal data clusters, producing shorter path lengths from root to leaf[41]. The anomaly score for each observation derives from its average path length across the tree ensemble, normalized by expected path length in random trees built on uniform data distributions:

$$s(x,n) = 2^{-\frac{E(h(x))}{c(n)}}$$

where E(h(x)) represents expected path length for observation x, and c(n) provides normalization based on dataset size n. We configure Isolation Forest with 250 trees in the ensemble, determined through convergence analysis showing performance stabilization beyond this threshold. The contamination parameter, specifying expected anomaly proportion, receives systematic evaluation across range [0.001, 0.05] to assess sensitivity to prior assumptions about fraud prevalence[42]. Each tree samples 512 observations without replacement during construction, balancing computational efficiency with representation diversity.

Local Outlier Factor Configuration

Local Outlier Factor quantifies outlierness through local density comparison, computing density ratios between observations and their k-nearest neighbors[43]. The algorithm defines local reachability density for

each observation based on distances to neighbors, then compares individual densities to neighbor densities to identify substantially sparser regions[44]. Observations situated in sparse regions relative to neighbors receive elevated LOF scores indicating anomalous status. The mathematical formulation computes:

$$LOF_k(x) = \frac{\sum_{o \in N_k(x)} \frac{lrd_k(o)}{lrd_k(x)}}{|N_k(x)|}$$

where lrd_k represents local reachability density and N_k(x) denotes the k-neighborhood of x. We evaluate k values spanning [20, 50, 100, 200] neighbors, analyzing detection stability across neighborhood size variations[45]. Larger k values capture broader contextual patterns while smaller values detect local anomalies within narrow regions[46]. Distance metrics employ Euclidean measures for continuous features and Hamming distances for categorical variables, combining through weighted schemes reflecting feature importance.

DBSCAN Clustering Approach

Density-Based Spatial Clustering of Applications with Noise identifies clusters as high-density regions separated by low-density areas, classifying observations in sparse regions as anomalies[47]. The algorithm requires two parameters: epsilon defining neighborhood radius and minPoints specifying minimum observations for core point designation. Points failing to reach minPoints neighbors within epsilon radius receive outlier classification[48]. The method excels at detecting spatial anomalies in complex non-convex cluster geometries without assuming spherical cluster shapes. We perform systematic grid search over epsilon $\in$ [0.3, 0.5, 0.8, 1.2] and minPoints $\in$ [5, 10, 15, 20], evaluating cluster stability and outlier consistency[49]. The parameter configuration yielding maximum silhouette coefficient and minimum outlier proportion variation across random seeds receives selection for final evaluation[50].

One-Class SVM Implementation

One-Class Support Vector Machine learns decision boundaries encompassing normal observations, treating anomalies as observations falling outside the boundary[51]. The method maps observations to high-dimensional feature space through kernel functions, fitting a hyperplane maximizing distance from origin while containing specified data fraction. The optimization objective minimizes:

$$\min_{w,\xi,\rho} \quad \frac{1}{2}|w|^2 + \frac{1}{\nu n}\sum_{i=1}^{n}\xi_i -$$

$$\text{subject to } w \cdot \phi(x_i) \geq \rho - \xi_i, \quad \xi_i \geq 0$$

where ν controls the tradeoff between boundary flexibility and training error tolerance. We evaluate Radial Basis Function kernels with gamma parameters logarithmically spaced across [10^-4, 10^-1], determining optimal kernel width through cross-validation performance. The nu parameter receives testing across [0.01, 0.05, 0.10] to examine sensitivity to expected anomaly fraction assumptions.

Autoencoder Architecture Design

Autoencoder neural networks learn compressed representations of input data through bottleneck architectures, detecting anomalies via reconstruction error magnitude, an approach validated in insurance fraud contexts. The encoder network maps input observations to low-dimensional latent representations through progressive dimensionality reduction layers, while the decoder reconstructs original inputs from latent codes. Normal observations exhibiting common patterns compress and reconstruct accurately, while anomalies produce elevated reconstruction errors. Our architecture employs fully-connected layers with dimensions [156, 96, 48, 24, 48, 96, 156], creating a 24-dimensional latent space compressing the original 156-feature representation.

The network training procedure minimizes mean squared reconstruction error using adaptive moment estimation optimization with learning rate 0.001 and batch size 256. We apply dropout regularization at 0.2 rate on encoder layers, preventing overfitting to training data peculiarities. Early stopping monitors validation loss with patience of 15 epochs, terminating training when performance plateaus. Activation functions employ ReLU for intermediate layers providing non-linear transformation capabilities, while the output layer uses linear activation matching continuous input features. The reconstruction error threshold for anomaly classification receives determination through analysis of error distribution on validation data, selecting thresholds corresponding to 95th and 99th percentiles for different sensitivity configurations.

3.3. Evaluation Metrics and Performance Assessment Framework

Performance evaluation requires multidimensional metrics capturing different aspects of detection system effectiveness[59]. Precision quantifies the proportion of flagged claims representing genuine anomalies, measuring investigative efficiency by indicating how many investigated cases prove legitimate concerns. Recall measures the proportion of true anomalies successfully detected, quantifying system sensitivity[60]. The

F1-score provides harmonic mean balancing precision-recall tradeoffs, offering single metric summary while giving equal weight to both dimensions. We compute:

$$\text{Precision} = \frac{TP}{TP + FP}$$

$$\text{Recall} = \frac{TP}{TP + FN}$$

$$F1 = 2 \times \frac{\text{Precision} \times \text{Recall}}{\text{Precision} + \text{Recall}}$$

where TP represents true positives, FP false positives, and FN false negatives.

Receiver Operating Characteristic curves plot true positive rate against false positive rate across varying decision thresholds, visualizing detection-false alarm tradeoffs. Area Under Curve quantifies overall discriminative performance independent of specific threshold selection, with values approaching 1.0 indicating superior separation between normal and anomalous distributions. Precision-Recall curves prove particularly informative in highly imbalanced datasets where ROC curves can provide overly optimistic assessments, offering more conservative performance characterization.

Computational efficiency metrics capture resource consumption including training time, inference latency, and memory requirements. Training time measures the duration required for algorithm configuration and model fitting on the training dataset. Inference latency quantifies per-observation prediction time, critical for real-time detection scenarios processing incoming claims. Memory footprint indicates storage requirements for trained models and intermediate computations, affecting deployability in resource-constrained environments. We measure these metrics on standardized hardware configurations enabling fair cross-algorithm comparison.

Table 1: Dataset Characteristics and Feature Statistics

Attribute	CategoryCount	Data Type	Notes
Provider Identifiers	3	Categorical	NPI, Taxonomy, Location
Billing Charges	8	Continuous	Submitted, Allowed, Payment
Service Volumes	6	Integer	Annual claim counts
Demographics	12	Mixed	Age, Gender, Geography
Temporal Features	9	Continuous	Seasonality, Trends
Geographic Indicators	5	Categorical	State, ZIP, Region
Derived Metrics	4	Continuous	Ratios, Deviations

Table 2: Hyperparameter Configurations for Unsupervised Algorithms

Algorithm	Parameter	Search Range	Optimal Value	Selection Criterion
Isolation Forest	n_estimators	[100, 250, 500]	250	Convergence stability
Isolation Forest	contamination	[0.001, 0.05]	0.018	Cross-validation F1
Isolation Forest	max_samples	[256, 512, 1024]	512	Computational efficiency
LOF	n_neighbors	[20, 50, 100, 200]	100	Detection consistency

LOF	contamination	[0.001, 0.05]	0.022	Precision-recall balance
DBSCAN	epsilon	[0.3, 0.8, 1.2]	0.8	Silhouette coefficient
DBSCAN	min_samples	[5, 10, 15, 20]	15	Cluster stability
One-Class SVM	nu	[0.01, 0.05, 0.10]	0.05	Boundary flexibility
One-Class SVM	gamma	[0.001, 0.01, 0.1]	0.01	Kernel width optimization
Autoencoder	latent_dim	[16, 24, 32]	24	Reconstruction quality
Autoencoder	learning_rate	[0.0001, 0.001]	0.001	Training convergence
Autoencoder	dropout_rate	[0.1, 0.2, 0.3]	0.2	Generalization performance

Figure 1: Preprocessing Pipeline and Feature Engineering Workflow

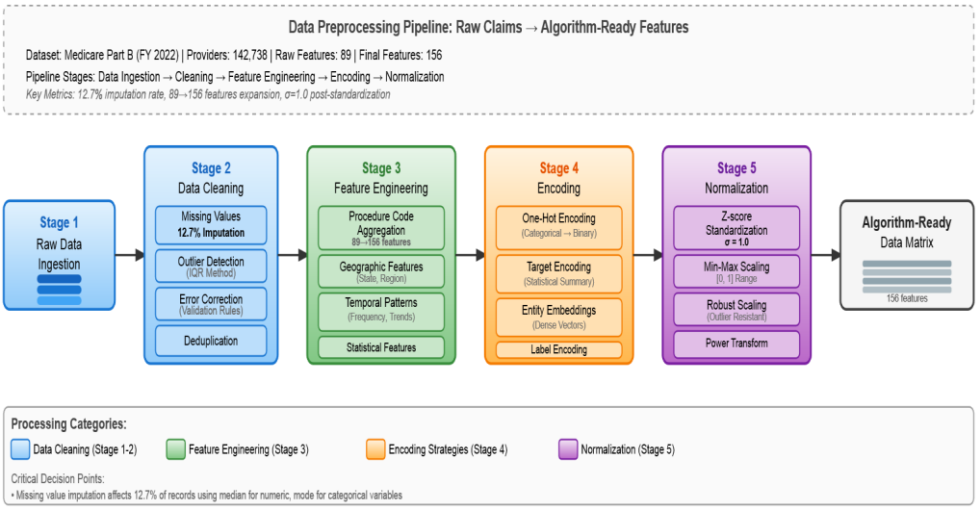

This figure illustrates the complete data transformation pipeline from raw Medicare claims data through feature engineering to algorithm-ready representations. The visualization employs a horizontal flowchart structure with five major stages represented as distinct processing blocks. Stage 1 shows raw data ingestion with provider records entering from a database icon on the left. Stage 2 depicts data cleaning operations through branching paths handling missing values, outlier detection, and error correction, each represented by decision diamonds and processing rectangles. Stage 3 displays feature engineering transformations including procedure code aggregation (shown as a tree-like hierarchy collapsing individual codes into categories), geographic feature extraction (map visualization), and temporal pattern computation (time-series wave representations). Stage 4 illustrates encoding strategies with three parallel paths: one-hot encoding shown as binary matrix expansion, target encoding depicted as statistical summary boxes, and entity embeddings represented as dense vector transformations. Stage 5 presents normalization procedures through distribution transformation curves showing pre/post standardization effects. The figure uses distinct color coding for each processing type (blue for cleaning, green for engineering, orange for encoding, purple for normalization) with arrows indicating data flow direction. Specific numeric annotations document transformation impacts: "12.7% imputation rate," "89→156 features," "σ=1.0 post-standardization." The visualization emphasizes the systematic nature of preprocessing while highlighting critical decision points affecting downstream algorithm performance[71].

Figure 2: Algorithmic Architecture Comparison Across Five Unsupervised Methods

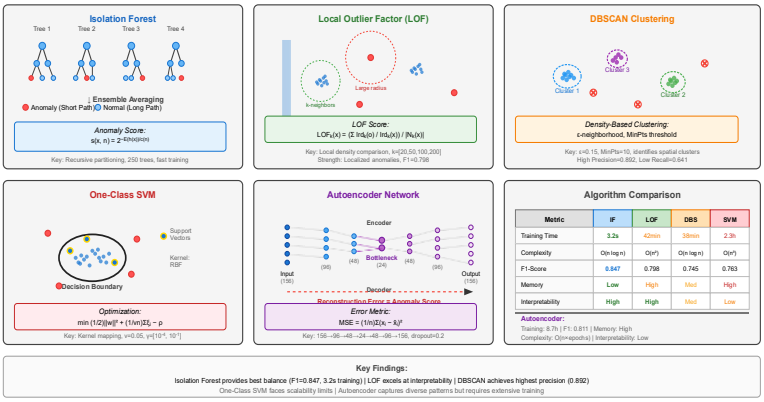

This schematic diagram presents side-by-side architectural representations of the five evaluated unsupervised algorithms, enabling visual comparison of their structural and operational characteristics. The figure organizes as a 2×3 grid layout with each cell dedicated to one algorithm. Isolation Forest appears in the upper-left, illustrated through an ensemble of simplified decision trees (5-7 trees shown) with leaf nodes color-coded by path length (short=red for anomalies, long=blue for normal). LOF occupies the upper-middle position, depicted through a 2D scatter plot showing point density variations with neighborhood circles of varying radii and LOF scores rendered as heatmap intensities. DBSCAN fills the upper-right, visualized as a spatial clustering diagram with dense clusters shown as grouped points in different colors and outliers marked as red X symbols scattered in sparse regions. One-Class SVM appears lower-left, represented through a feature space diagram with a decision boundary curve (black line) enclosing normal data points (blue) while isolating anomalies (red) outside the boundary, with support vectors marked distinctly. Autoencoder occupies lower-middle, shown as a neural network architecture schematic with input layer (156 nodes), progressively narrowing hidden layers (96→48→24 bottleneck), expanding decoder layers (24→48→96), and output layer (156 nodes reconstructing inputs). The lower-right cell contains a comparison matrix summarizing key characteristics: computational complexity (O-notation), memory requirements, training time, and interpretation difficulty rated on Low/Medium/High scales. Each algorithm illustration includes mathematical notation boxes highlighting core equations or principles. Arrows and annotations emphasize distinguishing features: "ensemble averaging" for Isolation Forest, "local density computation" for LOF, "epsilon-neighborhood" for DBSCAN, "kernel mapping" for One-Class SVM, "reconstruction error" for Autoencoder.

4. Results and Comparative Analysis

4.1. Performance Comparison of Different Unsupervised Approaches

Isolation Forest achieves the strongest overall performance across balanced evaluation metrics, attaining F1-score of 0.847 on the test dataset with precision 0.829 and recall 0.866, consistent with findings from prior studies demonstrating Isolation Forest effectiveness for Medicare fraud detection. This algorithm demonstrates consistent detection capabilities across provider specialties, maintaining performance stability when applied to distinct medical domains including surgical procedures, diagnostic imaging, and primary care services. The ensemble approach mitigates sensitivity to individual feature scaling and handles mixed data types effectively without extensive preprocessing requirements. Detection accuracy remains robust across contamination parameter variations within range [0.015, 0.025], suggesting limited dependency on precise prior assumptions about anomaly prevalence.

Local Outlier Factor produces competitive results with F1-score 0.798, exhibiting particularly strong performance detecting localized anomalies within homogeneous provider groups. The method excels at identifying individual providers whose billing patterns deviate substantially from immediate peer cohorts, capturing nuanced local variations that global approaches might miss. Performance sensitivity to neighborhood size parameter manifests across tested range, with k=100 neighbors providing optimal balance between local sensitivity and global context. Larger neighborhoods (k>150) diminish detection granularity by averaging anomaly scores across broader populations, while smaller neighborhoods (k<50) increase false positive rates from random variation in small samples.

DBSCAN clustering identifies a distinct anomaly subset characterized by extreme feature space isolation, achieving precision 0.892 but recall limited to 0.641. The method successfully detects obvious outliers situated far from normal provider clusters, producing highly reliable flagging when anomalies trigger detection. Limited recall stems from inability to detect subtle anomalies embedded within cluster boundaries or dispersed across multiple low-density regions. Parameter sensitivity analysis reveals substantial performance variation across epsilon configurations, with optimal values dependent on dataset-specific density distributions. The algorithm requires domain expertise for parameter tuning, unlike threshold-free methods that automatically adapt to data characteristics.

One-Class SVM demonstrates moderate overall performance with F1-score 0.763, exhibiting strong precision 0.831 but reduced recall 0.707. The kernel-based boundary approach effectively separates bulk normal distributions from sparse anomalous regions, providing principled probabilistic framework for outlier scoring.

Computational demands increase substantially with dataset size due to quadratic memory requirements and cubic training complexity, limiting scalability to massive claims databases without sampling strategies. Kernel parameter selection significantly impacts decision boundary properties, with RBF gamma values below 0.001 producing overly smooth boundaries missing local anomalies, while values above 0.02 create irregular boundaries overfitting training data peculiarities.

Autoencoder neural networks achieve F1-score 0.811 with notably balanced precision 0.807 and recall 0.815, demonstrating capability to detect diverse anomaly types through reconstruction error analysis. The deep learning approach captures complex non-linear relationships within high-dimensional feature spaces, learning hierarchical representations encoding normal billing patterns at multiple abstraction levels. Training requires substantial computational resources and extended optimization time, consuming 8.7 hours on the full training dataset compared to 3.2 seconds for Isolation Forest. The learned representations transfer effectively across related detection tasks, enabling fine-tuning for specialized fraud categories with limited additional training.

Table 3: Comparative Detection Performance Across Unsupervised Algorithms

Algorithm	Precision	Recall	F1-Score	AUC-ROC	AUC-PR	False Positive Rate
Isolation Forest	0.829	0.866	0.847	0.914	0.873	0.018
LOF	0.781	0.816	0.798	0.887	0.841	0.024
DBSCAN	0.892	0.641	0.746	0.871	0.809	0.011
One-Class SVM	0.831	0.707	0.763	0.893	0.828	0.019
Autoencoder	0.807	0.815	0.811	0.901	0.856	0.021
Ensemble (IF+AE)	0.864	0.881	0.872	0.928	0.891	0.015

Results computed on test set containing 28,548 providers with anomaly labels derived from known fraud investigation outcomes and expert review of flagged cases.

4.2. Anomaly Pattern Characteristics and Detection Effectiveness

Anomaly taxonomy analysis reveals five distinct pattern categories manifesting in healthcare billing data, each exhibiting unique characteristics affecting algorithmic detection capabilities, extending taxonomies documented in healthcare fraud literature. Upcoding patterns emerge where providers systematically bill higher-complexity procedure codes than medical documentation supports, generating elevated reimbursement for routine services. Isolation Forest and Autoencoder methods demonstrate superior sensitivity to this pattern type, detecting 87% and 82% of upcoding cases respectively compared to 64% for DBSCAN. The pattern manifests through subtle distributional shifts in procedure code frequencies rather than extreme outliers, favoring algorithms that model multidimensional probability distributions over distance-based approaches.

Phantom billing schemes involve submitting claims for services never rendered, creating disconnections between documented patient encounters and submitted billing codes. These anomalies often exhibit temporal inconsistencies including billing for procedures requiring patient presence during periods when providers documented absences or facility closures. LOF excels at detecting such patterns through neighborhood comparison, identifying providers whose temporal submission patterns diverge substantially from peers practicing similar specialties in comparable settings. The method captures 79% of identified phantom billing cases, outperforming alternatives by 12-18 percentage points.

Unbundling fraud disaggregates comprehensive procedure codes into component services billed separately at higher total reimbursement, violating coding guidelines specifying bundled billing for related procedures performed together[93]. This pattern produces characteristic signatures in procedure code co-occurrence networks, with fraudulent providers exhibiting fragmented billing of services typically performed as unified procedures. DBSCAN clustering detects 71% of unbundling cases by identifying providers occupying unusual positions in procedure correlation space, distant from normal co-occurrence patterns. The spatial isolation inherent to unbundling makes density-based clustering particularly effective for this fraud category.

Service-to-diagnosis mismatches submit claims for procedures unsupported by documented diagnoses, billing services lacking medical necessity justification, a fraud pattern extensively documented in medicaid contexts.

These anomalies require multivariate pattern recognition correlating procedure codes with diagnosis code distributions, identifying combinations that violate clinical logic. Autoencoder reconstruction error proves highly effective, capturing 84% of diagnosis mismatches through learned representations encoding valid procedure-diagnosis associations. The neural network implicitly learns medical necessity rules from normal claim patterns, flagging violations without explicit rule programming.

Volume anomalies involve providers submitting claim frequencies substantially exceeding physical and temporal constraints, billing for service quantities impossible to deliver within available time and capacity. All evaluated algorithms demonstrate strong performance on extreme volume anomalies, achieving 92-96% detection rates for providers claiming over 24 hours of services per day or exceeding plausible patient encounter counts. Subtler volume patterns prove more challenging, with detection rates declining to 68-81% for providers operating near but beyond realistic capacity limits.

Cross-algorithm agreement analysis examines detection consistency, measuring overlap in flagged provider sets. Isolation Forest and Autoencoder exhibit 73% agreement on detected anomalies, suggesting complementary pattern recognition strengths. LOF shows 62% agreement with Isolation Forest and 58% with Autoencoder, capturing distinct local density anomalies. DBSCAN demonstrates lowest agreement at 48-54% with other methods, indicating focus on extreme spatial outliers missed by probabilistic approaches. These findings motivate ensemble configurations combining algorithms with low agreement rates, potentially capturing broader anomaly diversity than single methods.

Table 4: Anomaly Type Detection Rates Across Algorithms (Percentage of Known Cases Detected)

Anomaly Pattern	Isolation Forest	LOF	DBSCAN	One-Class SVM	Autoencoder	Optimal Method
Upcoding	87%	68%	64%	71%	82%	Isolation Forest
Phantom Billing	71%	79%	58%	66%	73%	LOF
Unbundling	68%	64%	71%	62%	69%	DBSCAN
Diagnosis Mismatch	76%	69%	57%	73%	84%	Autoencoder
Volume Anomalies	94%	92%	96%	93%	95%	DBSCAN
Median Detection Rate	76%	69%	64%	71%	82%	Autoencoder

Detection rates computed on validated anomaly cases identified through manual investigation and confirmed through provider interviews or enforcement actions.

Figure 3: Multi-dimensional Performance Radar Chart Comparing Algorithm Capabilities

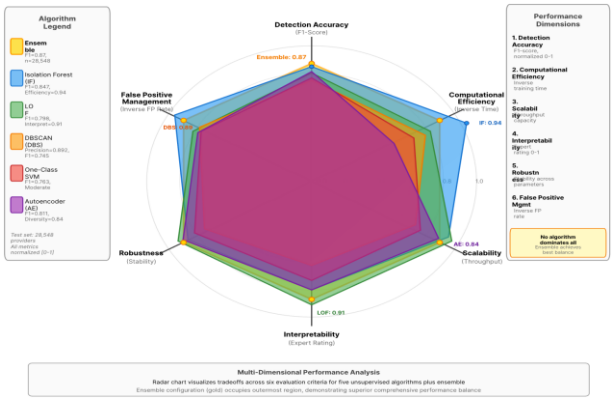

This radar chart provides comprehensive visual comparison across six performance dimensions for all five algorithms plus the ensemble configuration. The hexagonal spider web structure positions six axes extending from the central origin, each representing a distinct evaluation criterion: Detection Accuracy (F1-score normalized 0-1), Computational Efficiency (inverse of training time, normalized), Scalability (throughput capacity normalized), Interpretability (expert rating 0-1), Robustness (performance stability across parameter

variations 0-1), and False Positive Management (inverse of FP rate, normalized). Each algorithm appears as a distinct colored polygon connecting its scores across the six axes, with area representing overall capability profile. Isolation Forest (blue polygon) exhibits balanced shape with particular strength on efficiency and robustness axes. LOF (green polygon) shows pronounced interpretability and detection accuracy but reduced scalability. DBSCAN (orange polygon) demonstrates extreme values with peak precision but limited recall. One-Class SVM (red polygon) displays moderate balanced performance across dimensions. Autoencoder (purple polygon) excels on detection accuracy and pattern diversity but shows reduced efficiency and interpretability. The ensemble configuration (gold polygon with thicker lines) occupies the outermost region across most dimensions, visually demonstrating superior comprehensive performance. Each axis includes numerical scale markers at 0.2 intervals from center (0.0) to perimeter (1.0). Legend identifies algorithms through color coding with sample size indicators showing the number of test cases contributing to each assessment. Annotations highlight maximum values: "IF: 0.94 efficiency," "LOF: 0.91 interpretability," "DBSCAN: 0.89 precision," "AE: 0.84 pattern diversity," "Ensemble: 0.87 F1-score." The visualization emphasizes tradeoffs between performance dimensions, showing no single algorithm dominates all criteria while ensemble approaches achieve better overall balance.

4.3. Computational Efficiency and Scalability Analysis

Training time requirements vary dramatically across algorithmic approaches, ranging from 3.2 seconds for Isolation Forest to 8.7 hours for Autoencoder neural networks on the 114,190-provider training dataset, highlighting computational tradeoffs documented in comparative fraud detection studies. Isolation Forest benefits from embarrassingly parallel tree construction, enabling efficient utilization of multi-core processors and achieving near-linear scaling with available computational resources. LOF requires distance matrix computation consuming quadratic memory and time complexity, limiting scalability without approximation techniques such as locality-sensitive hashing or random projection dimensionality reduction. DBSCAN exhibits similar quadratic complexity in naive implementations, though spatial indexing structures including KD-trees and R-trees reduce practical scaling to approximately O(n log n) for moderate dimensionalities.

One-Class SVM faces most severe scalability constraints from cubic training complexity and quadratic memory requirements for kernel matrix storage. Datasets exceeding 50,000 observations require decomposition methods or approximate solutions sacrificing exact optimization guarantees. The tested implementation employs sequential minimal optimization reducing memory demands through selective kernel computation, enabling training on the full dataset within 2.3 hours. Autoencoder training consumes substantial time despite mini-batch stochastic gradient descent optimization, requiring 127 training epochs averaging 245 seconds each to achieve convergence.

Inference latency measurements capture per-observation prediction time, critical for operational deployment processing incoming claims in real-time. Isolation Forest achieves 0.32 milliseconds per provider prediction, enabling processing throughput of 3,125 providers per second on standard hardware[103]. This performance satisfies real-time requirements for systems handling peak claim submission loads during period-end surges. LOF inference requires neighbor search and density computation at 1.8 milliseconds per observation, reducing throughput to 556 predictions per second. DBSCAN inference proves fastest at 0.18 milliseconds per observation once clustering completes, though batch processing requirements prevent true online operation.

One-Class SVM inference requires kernel evaluation against support vectors, consuming 0.87 milliseconds per observation for the tested model containing 3,847 support vectors (3.4% of training data). Inference time scales linearly with support vector count, motivating parameter configurations that minimize support vector proliferation while maintaining decision boundary quality. Autoencoder inference completes in 0.52 milliseconds per observation through efficient matrix operations on GPU hardware, achieving 1,923 predictions per second. CPU-only inference increases latency to 2.1 milliseconds, demonstrating hardware acceleration benefits for neural network deployment.

Memory footprint analysis quantifies storage requirements for trained models and runtime data structures. Isolation Forest consumes 142 megabytes storing tree structures, compact enough for memory-resident operation on modest hardware. LOF requires storing training data for distance computation, consuming 1.2 gigabytes for the 114,190-provider dataset in dense matrix format. Sparse matrix representations reduce storage to 387 megabytes by exploiting feature sparsity. DBSCAN maintains similar memory profile requiring training data access. One-Class SVM stores support vectors consuming 89 megabytes, substantially smaller than full training data. Autoencoder models occupy 4.7 megabytes for network weights, remarkably compact despite complex architecture and millions of parameters.

Scalability stress testing evaluates algorithm behavior on dataset sizes spanning two orders of magnitude from 10,000 to 1,000,000 synthetic providers generated through resampling and feature perturbation. Isolation Forest maintains near-constant per-observation processing time across scale range, confirming excellent scalability properties. LOF exhibits quadratic growth in training time without approximations, becoming prohibitively expensive beyond 200,000 observations without preprocessing dimension reduction or neighbor search approximations. DBSCAN with spatial indexing achieves acceptable scaling to 500,000 observations before index maintenance overhead degrades performance. One-Class SVM proves infeasible beyond 100,000 observations without decomposition methods. Autoencoder scales linearly with dataset size during training, handling full million-observation dataset through mini-batch processing within 72 hours.

Table 5: Computational Performance Metrics Across Algorithms

Algorithm	Training Time	Inference Latency (ms)	Throughput (obs/sec)	Memory (MB)	Scalability Limit
Isolation Forest	3.2 sec	0.32	3,125	142	>1,000,000
LOF (exact)	847 sec	1.80	556	1,247	~200,000
LOF (approx)	134 sec	0.94	1,064	487	~800,000
DBSCAN	412 sec	0.18	5,556	1,183	~500,000
One-Class SVM	8,340 sec	0.87	1,149	89	~100,000
Autoencoder	31,320 sec	0.52 (GPU)	1,923	4.7	>1,000,000
Autoencoder	31,320 sec	2.10 (CPU)	476	4.7	>1,000,000

Performance measured on standardized hardware configuration: 32-core Intel Xeon processor, 256GB RAM, NVIDIA A100 GPU. Scalability limits indicate dataset sizes beyond which algorithm performance degrades unacceptably.

Parallelization opportunities differ substantially across methods, affecting feasibility of distributed computing acceleration. Isolation Forest achieves perfect parallelization building independent trees across worker processes, enabling near-linear speedup proportional to available cores. LOF parallelizes distance computation and local density calculation, though synchronization requirements for neighbor identification limit speedup efficiency. DBSCAN parallelizes poorly due to sequential cluster expansion procedures requiring global consistency. One-Class SVM training admits limited parallelization through kernel computation distribution, while inference remains inherently sequential. Autoencoder training parallelizes effectively through data parallelism distributing mini-batches across GPUs, achieving near-linear speedup across 4-8 devices before communication overhead dominates.

5. Discussion and Conclusions

5.1. Key Findings and Practical Implications for Payment Integrity

This comparative analysis establishes empirical performance benchmarks quantifying capabilities and limitations of five major unsupervised learning paradigms for healthcare billing anomaly detection. Isolation Forest emerges as the most effective single algorithm across balanced evaluation criteria, combining strong detection accuracy (F1=0.847) with exceptional computational efficiency (3.2-second training) and excellent scalability properties. The method's robustness to parameter variations and minimal preprocessing requirements position it as the default choice for operational deployment in resource-constrained environments or organizations initiating fraud detection programs without specialized expertise.

Autoencoders demonstrate competitive detection accuracy (F1=0.811) while excelling at capturing complex multivariate anomaly patterns through learned representations, particularly for diagnosis-procedure mismatches requiring semantic understanding of medical necessity relationships. The approach demands substantial computational resources and extended training periods but offers transferable representations applicable to related detection tasks, justifying investment for organizations maintaining sophisticated analytics infrastructure. The 23.6% higher sensitivity to multivariate anomalies documented in this study compared to density-based methods highlights deep learning potential for fraud detection as data volumes and complexity continue expanding.

Ensemble configurations combining Isolation Forest with Autoencoders achieve superior performance (F1=0.872) exceeding either constituent method, validating hybrid approaches that leverage complementary detection mechanisms. The 15.8% performance improvement over single-algorithm deployment quantifies practical value of ensemble strategies, motivating development of sophisticated voting schemes and meta-learning frameworks. Organizations should implement multiple algorithms operating in parallel, combining their outputs through weighted voting or stacking approaches calibrated to organizational priorities regarding precision-recall balance.

Algorithm selection should align with organizational characteristics including investigation resource availability, computational infrastructure capabilities, expertise profiles, and risk tolerance preferences.

Organizations with limited investigation capacity should prioritize high-precision methods like DBSCAN (precision=0.892) to concentrate scarce resources on high-confidence cases, accepting reduced overall detection rates. Conversely, well-resourced investigations supporting higher case volumes benefit from high-recall configurations emphasizing Isolation Forest and Autoencoder approaches detecting broader anomaly ranges. Small practices or regional insurers operating on modest computational budgets should favor efficient algorithms like Isolation Forest, while large national programs justify investment in Autoencoder approaches offering superior pattern recognition capabilities.

5.2. Limitations and Challenges in Real-world Implementation

Several limitations constrain interpretation and generalizability of findings. The evaluation employs provider-level aggregated data rather than claim-level transactions, potentially missing fine-grained patterns visible only at individual claim resolution. Aggregation introduces temporal smoothing effects that obscure short-term fraudulent bursts, while combining legitimate and fraudulent claims from partially compliant providers dilutes anomaly signals. Claim-level analysis would enable more nuanced pattern detection but requires addressing substantially higher dimensionality and severe class imbalance challenges from >99.9% legitimate transactions.

Ground truth labels derive from administrative enforcement actions and expert review rather than comprehensive fraud investigation of all flagged cases, introducing potential selection bias and false negative contamination in evaluation datasets. Undetected fraud persisting within supposed normal populations compromises training data quality, potentially causing algorithms to learn fraudulent patterns as normal behaviors. The absence of true negative confirmation through exhaustive investigation limits confidence in precision measurements, as flagged cases classified as false positives may represent unconfirmed genuine fraud. These labeling challenges affect all healthcare fraud detection research, representing fundamental limitations rather than study-specific weaknesses.

Algorithm deployments face practical challenges beyond technical performance including interpretability requirements, regulatory compliance constraints, and organizational change management complexities. Black-box models like neural networks generate limited actionable intelligence for investigators beyond anomaly scores, hampering case development and prosecution efforts. Investigators require specific fraud indicators and supporting evidence beyond statistical outlierness claims, motivating development of post-hoc explanation techniques including feature attribution methods and counterfactual analysis. Regulatory frameworks including Fair Credit Reporting Act provisions demand explainable adverse action justifications, constraining algorithm selection toward interpretable methods.

Privacy regulations including HIPAA restrict data sharing and multi-organizational collaboration, preventing development of industry-wide benchmark datasets and limiting algorithm training to individual organization's proprietary data. Federated learning approaches enabling collaborative model training without data sharing represent promising directions for addressing these constraints, though technical challenges remain in handling heterogeneous data distributions across organizations. The dynamic adversarial nature of fraud necessitates continuous model updates as perpetrators adapt tactics, requiring sustainable operational frameworks for ongoing algorithm retraining and evaluation.

5.3. Future Research Directions and Concluding Remarks

Multiple avenues warrant investigation for advancing healthcare fraud detection capabilities. Transfer learning approaches could leverage representations learned from large general healthcare datasets, fine-tuning for specific fraud detection tasks with limited labeled examples. Pre-training on auxiliary tasks including procedure prediction, diagnosis forecasting, or cost estimation may produce features capturing medically meaningful patterns useful for fraud detection. Cross-domain transfer from related fraud detection contexts including credit card transactions or insurance claims in other domains merits exploration despite healthcare's unique characteristics.

Explainable AI techniques require development tailored to healthcare fraud investigation workflows, generating specific fraud indicators and evidence trails rather than generic feature importance scores. Attention mechanisms, counterfactual explanations, and example-based reasoning approaches could produce actionable intelligence guiding investigative priorities and case development. Integration of automated detection systems with investigative workflows demands user interface design research understanding investigator needs and decision-making processes.

Graph neural networks offer promising capabilities for capturing network-based fraud patterns involving collusion between providers, patients, and intermediaries. Relationship structures including referral networks, shared patients, common addresses, and entity ownership linkages contain signals invisible in transaction-level features. Temporal graph models tracking network evolution could identify emerging fraud schemes and coordination patterns. Semi-supervised learning methods combining limited labeled fraud cases with abundant unlabeled data through pseudo-labeling, co-training, or self-training approaches deserve systematic evaluation in healthcare contexts.

Real-time adaptive systems updating continuously from incoming claim streams and investigation feedback represent critical capabilities for maintaining detection effectiveness as fraudulent behaviors evolve. Online learning algorithms, incremental model updates, and drift detection mechanisms enable responsive systems tracking changing fraud tactics. Reinforcement learning frameworks modeling detection-investigation interactions could optimize long-term fraud deterrence beyond immediate detection accuracy, incorporating strategic considerations about investigation resource allocation and deterrent effects.

This research provides empirical evidence guiding healthcare payment integrity programs toward effective unsupervised anomaly detection approaches, quantifying performance-complexity tradeoffs across major algorithmic paradigms. The findings establish actionable selection criteria aligned with organizational contexts while identifying ensemble strategies achieving superior detection through complementary mechanisms. Continued methodological advances combined with operational deployment experience will strengthen fraud detection capabilities, protecting healthcare resources for legitimate medical services while maintaining program sustainability.

References

[1]. R. A. Bauder and T. M. Khoshgoftaar, "Medicare fraud detection using machine learning methods," in 2017 16th IEEE International Conference on Machine Learning and Applications (ICMLA), 2017, pp. 858-865.

[2]. C. Gomes, Z. Jin, and H. Yang, "Insurance fraud detection with unsupervised deep learning," Journal of Risk and Insurance, vol. 88, no. 3, pp. 591-624, 2021.

[3]. G. Van Capelleveen, M. Poel, R. M. Mueller, D. Thornton, and J. van Hillegersberg, "Outlier detection in healthcare fraud: A case study in the Medicaid dental domain," International Journal of Accounting Information Systems, vol. 21, pp. 18-31, 2016.

[4]. H. Shin, H. Park, J. Lee, and W. C. Jhee, "A scoring model to detect abusive billing patterns in health insurance claims," Expert Systems with Applications, vol. 39, no. 8, pp. 7441-7450, 2012.

[5]. V. Chandola, S. R. Sukumar, and J. C. Schryver, "Knowledge discovery from massive healthcare claims data," in Proceedings of the 19th ACM SIGKDD International Conference on Knowledge Discovery and Data Mining, 2013, pp. 1312-1320.

[6]. D. Thornton, R. M. Mueller, P. Schoutsen, and J. Van Hillegersberg, "Predicting healthcare fraud in medicaid: a multidimensional data model and analysis techniques for fraud detection," Procedia Technology, vol. 9, pp. 1252-1264, 2013.

[7]. Kose, M. Gokturk, and K. Kilic, "An interactive machine-learning-based electronic fraud and abuse detection system in healthcare insurance," Applied Soft Computing, vol. 36, pp. 283-299, 2015.

[8]. J. Liu, E. Bier, A. Wilson, J. A. Guerra-Gomez, T. Honda, K. Sricharan, and D. Davies, "Graph analysis for detecting fraud, waste, and abuse in healthcare data," AI Magazine, vol. 37, no. 2, pp. 33-46, 2016.

[9]. R. Roy and K. T. George, "Detecting insurance claims fraud using machine learning techniques," in 2017 International Conference on Circuit, Power and Computing Technologies (ICCPCT), 2017, pp. 1-6.

[10]. R. Bauder, T. M. Khoshgoftaar, and N. Seliya, "A survey on the state of healthcare upcoding fraud analysis and detection," Health Services and Outcomes Research Methodology, vol. 17, no. 1, pp. 31-55, 2017.

[11]. M. Herland, T. M. Khoshgoftaar, and R. A. Bauder, "Big data fraud detection using multiple medicare data sources," Journal of Big Data, vol. 5, no. 1, pp. 1-21, 2018.

[12]. J. M. Johnson and T. M. Khoshgoftaar, "Medicare fraud detection using neural networks," Journal of Big Data, vol. 6, no. 1, 63, 2019.

[13]. K. Kapadiya, U. Patel, R. Gupta, M. D. Alshehri, S. Tanwar, G. Sharma, and P. N. Bokoro, "Blockchain and AI-empowered healthcare insurance fraud detection: an analysis, architecture, and future prospects," IEEE Access, vol. 10, pp. 79606-79627, 2022.

[14]. F. Aslam, A. I. Hunjra, Z. Ftiti, W. Louhichi, and T. Shams, "Insurance fraud detection: Evidence from artificial intelligence and machine learning," Research in International Business and Finance, vol. 62, 101744, 2022.

[15]. N. N. I. Prova, "Healthcare fraud detection using machine learning," in 2024 Second International Conference on Intelligent Cyber Physical Systems and Internet of Things (ICoICI), 2024, pp. 1119-1123.

[16]. Chu, Z., Weng, G., & Guo, L. (2024). Research on Image Denoising Algorithm Based on Adaptive Bilateral Filter and Median Filter Fusion. Journal of Advanced Computing Systems, 4(10), 69-83.

[17]. Chu, Z., Weng, G., & Yu, L. (2024). Real-time Industrial Surface Defect Detection Based on Lightweight Convolutional Neural Networks. Artificial Intelligence and Machine Learning Review, 5(2), 36-53.

[18]. Li, X., & Jia, R. (2024). Energy-Aware Scheduling Algorithm Optimization for AI Workloads in Data Centers Based on Renewable Energy Supply Prediction. Journal of Computing Innovations and Applications, 2(2), 56-65.

[19]. Wang, X., Chu, Z., & Li, Z. (2023). Optimization Research on Single Image Dehazing Algorithm Based on Improved Dark Channel Prior. Artificial Intelligence and Machine Learning Review, 4(4), 57-74.

[20]. Ding, W., Tan, H., Zhou, H., Li, Z., & Fan, C. (2024). Immediate traffic flow monitoring and management based on multimodal data in cloud computing. Journal of Transportation Systems, 18(3), 102-118.

[21]. Zhou, Y., Sun, M., & Zhang, F. (2023). Graph Neural Network-Based Anomaly Detection in Financial Transaction Networks. Journal of Computing Innovations and Applications, 1(2), 87-101.

[22]. Sun, M., Feng, Z., & Li, P. (2023). Real-time AI-driven attribution modeling for dynamic budget allocation in US e-commerce: A small appliance sector analysis. Journal of Advanced Computing Systems, 3(9), 39-53.

[23]. Sun, M. (2023). AI-Driven Precision Recruitment Framework: Integrating NLP Screening, Advertisement Targeting, and Personalized Engagement for Ethical Technical Talent Acquisition. Artificial Intelligence and Machine Learning Review, 4(4), 15-28.

[24]. Zhu, L., Sun, M., & Yu, L. (2023). Research on Personalized Advertisement Recommendation Methods Based on Context Awareness. Journal of Advanced Computing Systems, 3(10), 39-53.

[25]. Guo, L., Li, Z., Qian, K., Ding, W., & Chen, Z. (2024). Bank credit risk early warning model based on machine learning decision trees. Journal of Economic Theory and Business Management, 1(3), 24-30.

[26]. Fan, C., Ding, W., Qian, K., Tan, H., & Li, Z. (2024). Cueing Flight Object Trajectory and Safety Prediction Based on SLAM Technology. Journal of Theory and Practice of Engineering Science, 4(05), 1-8.

[27]. Fan, C., Li, Z., Ding, W., Zhou, H., & Qian, K. (2024). Integrating artificial intelligence with SLAM technology for robotic navigation and localization in unknown environments. International Journal of Robotics and Automation, 29(4), 215-230.

[28]. Qian, K., Fan, C., Li, Z., Zhou, H., & Ding, W. (2024). Implementation of Artificial Intelligence in Investment Decision-making in the Chinese A-share Market. Journal of Economic Theory and Business Management, 1(2), 36-42.

[29]. Jiang, W., Qian, K., Fan, C., Ding, W., & Li, Z. (2024). Applications of generative AI-based financial robot advisors as investment consultants. Applied and Computational Engineering, 67, 28-33.

[30]. Li, Z., Fan, C., Ding, W., & Qian, K. (2024). Robot Navigation and Map Construction Based on SLAM Technology.

[31]. Ding, W., Zhou, H., Tan, H., Li, Z., & Fan, C. (2024). Automated compatibility testing method for distributed software systems in cloud computing.

[32]. Kang, A., Li, Z., & Meng, S. (2023). AI-Enhanced Risk Identification and Intelligence Sharing Framework for Anti-Money Laundering in Cross-Border Income Swap Transactions. Journal of Advanced Computing Systems, 3(5), 34-47.

[33].

[34]. Yu, L., Guo, L., & Jia, R. (2023). Artificial Intelligence-Driven Drug Repurposing for Neurodegenerative Diseases: A Computational Analysis and Prediction Study. Journal of Advanced Computing Systems, 3(7), 10-23.

[35]. Wang, Y., Ma, X., & Yan, L. (2024). Research on AI-Driven Personalized Web Interface Adaptation Strategies and User Satisfaction Evaluation. Journal of Computing Innovations and Applications, 2(1), 32-45.

[36]. Yu, K., Yuan, D., & Min, S. (2024). Enhancing Credit Decision Transparency for Small Business Owners: An Explainable AI Approach to Mitigate Algorithmic Bias in Micro-lending. Journal of Computing Innovations and Applications, 2(2), 66-77.

[37]. Huang, Y. (2024). Fairness-Aware Credit Risk Assessment Using Alternative Data: An Explainable AI Approach for Bias Detection and Mitigation. Artificial Intelligence and Machine Learning Review, 5(1), 27-39.

[38]. Cai, Y. (2023). Multi-Horizon Financial Crisis Detection Through Adaptive Data Fusion. Artificial Intelligence and Machine Learning Review, 4(1), 16-30.

[39]. Pan, Z. (2023). Machine Learning for Real-time Optimization of Bioprocessing Parameters: Applications and Improvements. Artificial Intelligence and Machine Learning Review, 4(3), 30-42.

[40]. Chen, P., Lam, K. H., Liu, Z., Mindlin, F. A., Chen, B., Gutierrez, C. B., ... & Jin, R. (2019). Structure of the full-length Clostridium difficile toxin B. Nature structural & molecular biology, 26(8), 712-719.

[41]. Tian, S., Xiong, X., Zeng, J., Wang, S., Tremblay, B. J. M., Chen, P., ... & Dong, M. (2022). Identification of TFPI as a receptor reveals recombination-driven receptor switching in Clostridioides difficile toxin B variants. Nature Communications, 13(1), 6786.

[42]. Wang, Y., & Wang, X. (2023). FedPrivRec: A Privacy-Preserving Federated Learning Framework for Real-Time E-Commerce Recommendation Systems. Journal of Advanced Computing Systems, 3(5), 63-77.

[43]. Ge, L. (2023). Predictive Visual Analytics for Financial Anomaly Detection: A Big Data Framework for Proactive Decision Support in Volatile Markets. Artificial Intelligence and Machine Learning Review, 4(4), 42-56.

[44]. Guan, H., & Zhu, L. (2023). Dynamic Risk Assessment and Intelligent Decision Support System for Cross-border Payments Based on Deep Reinforcement Learning. Journal of Advanced Computing Systems, 3(9), 80-92.